Biophysical Chemistry 19 (1984) 245–253
Elsevier

BPC 00842

THE INTERACTIONS BETWEEN NUCLEIC ACIDS AND POLYAMINES

III. MICROSCOPIC PROTONATION CONSTANTS OF SPERMIDINE

Frederick ONASCH [a], David AIKENS [a], Stanley BUNCE *[a], Herbert SCHWARTZ [a], Dean NAIRN [b] and Charles HURWITZ [c]

[a] *Department of Chemistry and* [b] *Computer Services, Rensselaer Polytechnic Institute, Troy, NY 12181, and* [c] *Veterans Administration Hospital, Albany, NY 12208, U.S.A.*

Received 15th August 1983
Revised manuscript received 9th September 1983
Accepted 10th November 1983

Key words: Basicity; Spermidine; Microprotonation constant; Two-dimensional NMR

Changes in the NMR chemical shifts of protons adjacent to the nitrogen atoms of spermidine which are undergoing protonation have been measured by two-dimensional heteronuclear coupled NMR. Data thus obtained measure the dependence of the state of protonation of individual nitrogens on the pH, and permit calculation of the microprotonation constants of spermidine and the concentrations of all of the variously protonated spermidine species present at any pH.

1. Introduction

The central role of spermidine in biochemical processes has led to considerable interest in establishing its protonation sequence. This property derives its significance from the general recognition that many of the biochemical functions of spermidine almost certainly depend on the charge distribution of partially protonated species and on the hydrogen bonding ability or acidity of the protonated base centers. Attempts to establish this aspect of spermidine's chemistry by ^{13}C-NMR [1–3], by thermochemical studies [4,5] and by ^{15}N-NMR [3] are in some disagreement, and the values of the microscopic protonation constants have not been reported.

If the individual base sites of a polybasic molecule differ sufficiently in basicity, they are protonated sequentially, with each site being essentially fully protonated before the next is protonated significantly. In spermidine, however, all three base sites are of comparable basicity. There are multiple parallel protonation pathways, and at each point in the protonation sequence a number of base sites are protonated to a significant degree. Determination of the microscopic protonation constants then requires an experimental measure of the extent of protonation of each base site that is insensitive to the extent of protonation of the others. The first study of microscopic protonation constants employed ultraviolet absorbance [6], but most recent studies are based on NMR chemical shift measurements. Previous studies of the protonation of spermidine have employed ^{13}C-NMR and ^{15}N-NMR [1–3], but both of these techniques have significant limitations. ^{13}C-NMR is troubled by long-range effects in that protonation of a given base center affects the chemical shifts of carbons as much as five centers distant [7]. ^{15}N-NMR is somewhat influenced by long-range effects [8] and it requires either isotopic enrichment

* To whom correspondence should be addressed.

or high sample concentrations. For example, in their recent study, Takeda et al. [3] used a spermidine concentration of 1.57 M.

In contrast to the limited use of ^{13}C-NMR and ^{15}N-NMR, ^{1}H-NMR has proven to be very effective for determining the protonation sequence of a number of types of compounds including amino acids, tetracycline antibiotics and chelating agents [9–12]. A major advantage of ^{1}H-NMR over ^{13}C-NMR is that proton chemical shift changes with protonation are largest at α-carbons, and decrease rapidly with distance from the protonation site. Thus, the chemical shift of the methylene protons adjacent to a given base center constitutes a nearly ideal measure of the extent of its protonation [12–14]. Unfortunately, direct application of ^{1}H-NMR spectroscopy to determining the protonation sequence of spermidine appears to be virtually impossible at present, since the proton chemical shifts of the four methylene groups adjacent to the base sites of spermidine differ by only 0.12 ppm [15], a difference far too small to permit their resolution by conventional ^{1}H-NMR, even at high frequency.

Two-dimensional ^{1}H-^{13}C correlated NMR spectroscopy affords an attractive solution to this problem [15]. Using this technique we have resolved the resonances of all the α-methylene protons of spermidine between pH 5 and 13, and have analyzed the resultant ^{1}H-NMR titration curves to obtain the complete set of microscopic protonation constants. In essence, the two-dimensional technique correlates each proton with the carbon to which it is bonded and separates proton resonances according to the chemical shifts of the corresponding carbons. Because the chemical shifts of the carbons span a much wider range than do those of the corresponding protons, the resolution is much better than that obtainable by conventional ^{1}H-NMR. The principal limitation is that because of the relatively low sensitivity of ^{13}C-NMR it is necessary to use a spermidine concentration of 0.1 M. At this concentration the ionic strength of the test solution changed substantially over the course of protonation, which required that we modify the method for calculating the H^+ concentration from the measured pH.

2. Notation

Our notation for spermidine (I), which is shown below, uses the notation of Kimberley and Goldstein [2] for the nitrogens. The stepwise macroscopic protonation constants are denoted K_1, K_2 and K_3. Microscopic constants are denoted by lower-case k terms, with subscripts to indicate the sites of protonation, where the current proton added is indicated by the last subscript.

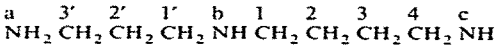

(I)

3. Materials and Methods

3.1. Source and purification

Spermidine was obtained commercially as the trihydrochloride salt and purified by recrystallization thrice from 80–95% aqueous ethanol. It was free of detectable impurities as judged by TLC [16].

3.2. Definition of $p[H^+]$

Values of $p[H^+]$, the concentration-based pH, needed for the curve-fitting analysis, were obtained in the following manner. The Corning Model 135 digital pH meter was calibrated at 25 ± 0.05°C using the NBS * standard buffers, and all pH measurements were performed at this temperature. To compensate for the effect of the 10% $^{2}H_2O$ content of the solutions used for NMR measurements, 0.04 pH unit was added to each such measured pH value. The ionic strength of the 0.1 M spermidine hydrochloride solutions, which ranges from 0.3 for the completely neutralized material ($\bar{n} = 0$) to 0.6 for the trihydrochloride ($\bar{n} = 3$), is too high to estimate the $p[H^+]$ by the method of Hedwig and Powell [17,18]. Instead, we used a version of the Davies equation [19] to estimate the activity coefficient of H^+ in 0.1 M spermidine hydrochloride at various stages of neutralization. Eq. 1, for which the regression coeffi-

* NBS, National Bureau of Standards.

cient is 1.000, reports the relationship of $p[H^+]$ to pH established in this manner.

$$p[H^+] = (pH + 0.04393)/1.0045 \quad (1)$$

3.3 NMR spectroscopy

Proton spectra were secured by the two-dimensional ^1H-^{13}C correlated NMR technique described in the review by Bax [20]. In summary, this procedure uses paired pulse sequences [21]. The sequence for ^1H is $90°-t_1-90°$-decouple, where t_1 is the delay time. From the same initial time, the pulse sequence for ^{13}C follows a $-t_{1/2}-180°-t_{1/2}-90°$ sequence, where $t_{1/2}$ is $t_1 \div 2$. The interaction of excited ^1H and ^{13}C nuclei results in the encoding of the ^1H spectra in the ^{13}C spectra from which the two-dimensional spectra are generated. 256 individual ^{13}C spectra of 128 transients each were taken with the delay time t_1 being incremented between spectra. The spectral variation with respect to the change in t_1 becomes the basis for the Fourier transformation in the second dimension. The resulting-two-dimensional spectra contain ^1H chemical shift information along one axis (^{13}C sweep width = 2400 Hz). A typical contour plot is shown in fig. 1. Precise proton chemical shifts were determined digitally by the XL-200 computer processor. They were verified by hand positioning a cursor on CRT displays of the optimized spectra. 1024 digitized points were used for the ^{13}C dimension and the ^1H dimension was zero-filled to 512 points. Exponential line broadening of 1.0–1.5 Hz was used in both dimensions. A Varian XL-200 NMR spectrometer with standard hardware and software was used; operating frequencies were 200 MHz for ^1H and 50 MHz for ^{13}C. A spermidine concentration of 0.1 M in 10% $^2H_2O/H_2O$ with dioxane as an internal standard was used throughout. The sample volume was approx. 2.4 ml, the tube diameter 10 mm and the probe temperature 20 ± 1°C.

Chemical shifts of the four α protons of 26 samples, from pH 5.89 to 13.33, were measured in this way. The total proton chemical shift change was 0.439 ppm at C-4, 0.490 at C-3′, 0.580 at C-1 and 0.600 at C-1′. The normalized values of these changes for protons at C-4, C-3′ and C-1 were

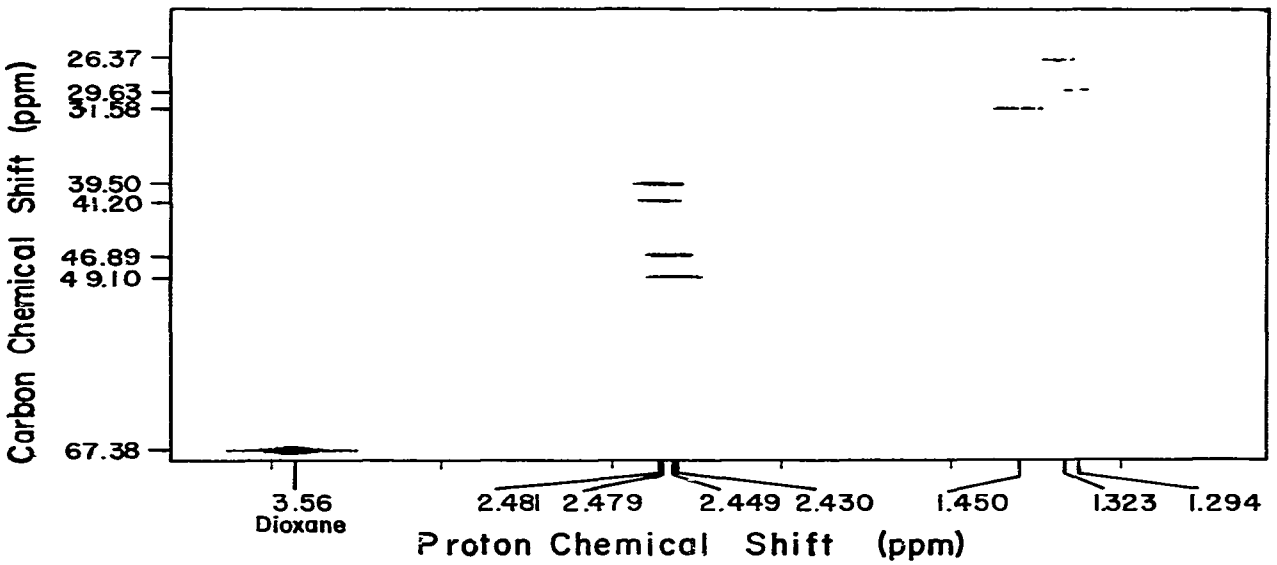

Fig. 1. Two-dimensional plot of chemical shifts (relative to tetramethylsilane (TMS)) of carbons and associated protons of spermidine; pH 11.296, 0.10 M.

used in the calculation of microscopic constants, and are plotted in fig. 2.

4. Data analysis

4.1. Curve-fitting considerations

The method we used to estimate the microscopic protonation constants of spermidine from chemical shift-pH data is based on that used by Hedwig and Powell [17,18] to estimate macroscopic constants of polyamines by fitting $\bar{n}$ vs. p[H^+] plots. There are, however, three factors which cause determination of the microscopic constants of spermidine to be more difficult than that of its macroscopic constants. First, there are only three macroscopic protonation constants, but there are 12 microscopic protonation constants. Second, the microscopic constants are related to the macroscopic constants, increasing the number of adjustable parameters to 15. When the number of adjustable parameters is this large, curve-fitting methods lose much of their value. That is, the derived constants may exhibit an excellent fit statistically, but their physical significances becomes questionable. Finally, determining the microscopic constants requires simultaneous fitting of three $\bar{n}$ vs. p[H^+] plots.

4.2. Curve-fitting method

Our approach to this problem has been to fit the constants in three steps. In the first step, we determine the three microscopic constants for adding the first proton, the three macroscopic protonation constants, and complex combinations of the remaining microscopic constants. In a second step, we determine the three microscopic constants for adding the last proton, the three macroscopic protonation constants, and complex combinations of the remaining microscopic constants. The last step is to calculate the six microscopic constants for adding the second proton by using the relationships which link them to the previously established microscopic and macroscopic protonation constants.

A brief outline of this approach showing the form of the equations fitted to the data is given below, using nitrogen N-a as an example. Making the substitutions below in the conventional equations for $\bar{n}_a$ and $\bar{h}_a$ reduces the number of adjustable parameters and yields eqs. 2 and 3.

$$A = k_a(k_{ab} + k_{ac})$$

$$B = k_b(k_{ba} + k_{bc})$$

$$C = k_c(k_{ca} + k_{cb})$$

$$D = K_1K_2K_3$$

$$0.5(A + B + C) = K_1K_2$$

$$A' = k_{cba}^{-1}(k_{cb}^{-1} + k_{bc}^{-1})$$

$$B' = k_{acb}^{-1}(k_{ca}^{-1} + k_{ac}^{-1})$$

$$C' = k_{abc}^{-1}(k_{ba}^{-1} + k_{ab}^{-1})$$

$$D' = (K_1^{-1}K_2^{-1}K_3^{-1})$$

$$0.5(A' + B' + C') = (K_2K_3)^{-1}$$

$$\bar{n}_a = \frac{k_a[H^+] + A[H^+]^2 + D[H^+]^3}{1 + K_1[H^+] + 0.5(A + B + C)[H^+]^2 + D[H^+]^3} \quad (2)$$

$$\bar{h}_a = \frac{k_{bca}^{-1}[H^+]^2 + A'[H^+] + D'}{[H^+]^3 + K_3^{-1}[H^+]^2 + 0.5(A' + B' + C')[H^+] + D'} \quad (3)$$

Simultaneously fitting eq. 2 and the corresponding expressions for $\bar{n}_b$ and $\bar{n}_c$ to the experimental values of $\bar{n}_a$, $\bar{n}_b$ and $\bar{n}_c$ yields K_1, K_2, K_3, k_a, k_b and k_c. In a similar manner, simultaneously fitting eq. 3 and the corresponding expressions for $\bar{h}_b$ and $\bar{h}_c$ to the experimental values of $\bar{h}_a$, $\bar{h}_b$ and $\bar{h}_c$ yields K_1, K_2 and K_3 again along with k_{bca}, k_{acb} and k_{abc}.

To fit these equations to the data, we used the so-called elliptical algorithm, also known as the space constriction method [22–26]. The elliptical algorithm is a type of nonlinear least-squares technique which is slower than that based on Newton's method, but more successful in finding unique solutions to curve-fitting problems.

5. Results

Fig. 2 reports the dependence on p[H^+] of the chemical shifts of the protons α to the three base sites of spermidine. To minimize the influence of long-range effects, the chemical shift of the protons of C-1 was used to monitor protonation of

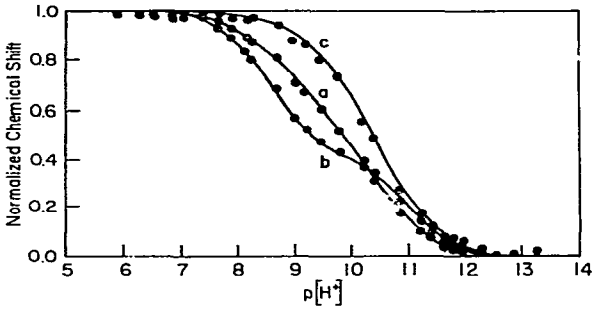

Fig. 2. Normalized chemical shift vs. p[H^+] plots for protons α to N-a, N-b and N-c of spermidine. The data for N-b refer to C-1. The letter next to each curve indicates the base site. The limiting proton shift values for each base site in ppm relative to TMS are as follows: N-a, 2.929, 2.439; N-b, 2.935, 2.355; N-c, 2.853, 2.414.

Table 2

Microscopic protonation constants of spermidine

Constant	log k [a]
k_a	10.42
k_b	10.58
k_c	10.61
k_{ab}	9.56
k_{ac}	10.37
k_{ba}	9.41
k_{bc}	10.01
k_{ca}	10.18
k_{cb}	9.98
k_{abc}	9.57
k_{acb}	8.76
k_{cba}	8.97

[a] The SOS term is the same as for the NMR-based constants in Table 1.

nitrogen N-b. The scatter at the high-p[H^+] end of the plots appears to be random as replicate values secured after analysis of the data and not included in the plot exhibit significantly less scatter.

The values of the macroscopic and microscopic protonation constants of spermidine derived from the NMR titration curves of fig. 2 are in tables 1 and 2, respectively. For comparison, table 1 also reports the macroscopic protonation constants derived using the method of Hedwig and Powell [17,18] from the conventional pH titration of spermidine under conditions similar to those of the nmr measurements. The six microscopic constants governing the addition of the second proton were not determined by curve fitting, but rather from the relationships linking them to the three macroscopic constants and the six other microscopic constants, all of which had been determined by curve fitting. Strictly speaking, therefore, the statistical estimates of the goodness of fit in table 2 do not apply to the six microscopic constants defining the addition of the second proton. The smooth curves of fig. 2 are derived from the entire set of microscopic constants, and across the entire pH range the agreement between these curves and the data points appears to be equally good. As indicated by the sum of squares term, the potentiometric titration data fit the macroscopic constants significantly better than do the NMR titration data. We suspect that a significant factor is that the temperature control for the NMR measurements was relatively poor (± 1°C) relative to that for the potentiometric measurements (± 0.05°C).

Table 1

Macroscopic protonation constants of spermidine

Source	log K_1	log K_2	log K_3	SOS [d]
pH titration [a,b]	10.96	9.91	8.51	7.5×10^{-3}
NMR [a,c]	11.02	10.02	8.57	1.87×10^{-2}

[a] Spermidine concentration, 0.1 M.
[b] $T = 25.0 \pm 0.05$°C.
[c] $T = 20 \pm 1$°C.
[d] SOS = $(\bar{n}_{i,obs} - \bar{n}_{i,calc})^2$; the number of $\bar{n}_i$ values is 81.

6. Discussion

6.1. Comparison with earlier work

Three earlier groups [1–3] have established certain aspects of the protonation sequence of spermidine. Even though differences in temperature and ionic strength among the various studies preclude quantitative comparison, the conclusions differ sufficiently that qualitative comparisons are of value.

Kimberley and Goldstein's [2] conclusions, which pertain to ^{13}C-NMR at 31°C over a range

of spermidine concentrations, agree closely with ours, which refer to a spermidine concentration of 0.1 M at 20°C. Their values of the macroscopic protonation constants for 0.078 M spermidine differ from our value for 0.1 M spermidine by no more than 0.16 log units, and their estimates of the fraction of each site protonated in 0.037 M spermidine at the monoprotonated and diprotonated stages agree relatively well with the values derived from our microscopic protonation constants. They estimate $\bar{n}_c$, $\bar{n}_b$ and $\bar{n}_c$ in monoprotonated spermidine to be 0.32, 0.32 and 0.43, respectively, as compared to our estimates of 0.28, 0.30 and 0.41. The agreement is nearly as good for diprotonated spermidine, for which Kimberley and Goldstein's estimates of $\bar{n}_a$, $\bar{n}_b$ and $\bar{n}_c$ are 0.67, 0.42 and 0.86 and our estimates are 0.64, 0.50 and 0.86.

In contrast to Kimberley and Goldstein's results and ours, Delfini et al. [1] concluded from their ^{13}C-NMR study that N-a and N-c are equally basic and that up to and including the diprotonated stage, protonation occurs only at these two sites. That is, in monoprotonated spermidine, the values of $\bar{n}_a$, $\bar{n}_b$ and $\bar{n}_c$ are 0.50, 0.00 and 0.50, respectively, while in diprotonated spermidine, they are 1.00, 0.00 and 1.00.

The conclusions of Takeda et al. [3], which are based on both ^{13}C-NMR and ^{15}N-NMR of 1.57 M spermidine, also differ substantially from ours. The macroscopic protonation constants they derived from ^{15}N-NMR data agree reasonably well with those they derived from ^{13}C-NMR data, but are larger than ours by between 0.5 and 1.0 log units. However, their estimates of the macroscopic protonation constants determined by potentiometric titration of spermidine in a 0.1 ionic strength medium are significantly lower, and in good agreement with those of other workers [2,17,18,27]. They suggested that at the high spermidine concentration in their NMR studies, intermolecular interactions may enhance the apparent basicity. With respect to the protonation sequence, they propose that the first equivalent of protons binds exclusively at N-c, the second at N-a and the third at N-b. That is, at the monoprotonated stage, $\bar{n}_a$, $\bar{n}_b$ and $\bar{n}_c$ are 0.0, 0.0 and 1.0, respectively, and at the diprotonated stage the corresponding values are 1.0, 0.0 and 1.0.

A source of guidance in evaluating the various protonation schemes proposed for spermidine is the set of microscopic protonation constants for spermidine derived from the protonation constants of model compounds [27]. These values, which apply to an ionic strength of 0.1 and a temperature of 25°C, predict that in monoprotonated spermidine $\bar{n}_a$, $\bar{n}_b$ and $\bar{n}_c$ are 0.28, 0.31 and 0.40, respectively, in excellent agreement with the values of 0.28, 0.31 and 0.41 calculated from the microscopic constants we derived experimentally in the present work. For diprotonated spermidine, the agreement is not as good, the predicted values of $\bar{n}_a$, $\bar{n}_b$ and $\bar{n}_c$ being 0.75, 0.36 and 0.89, respectively, as compared to values of 0.64, 0.50 and 0.86 derived from our experimental microscopic constants. Considering the simplicity of the model and the difference between the conditions to which the model and the experimental refer, the overall agreement between the calculated and measured sets of $\bar{n}$ values is quite reasonable, and it constitutes strong if indirect support for our values of the microscopic protonation constants of spermidine.

6.2. *Protonation sequence*

Establishment of the microscopic protonation constants allows calculation of the complete protonation sequence of spermidine. The protonation sequence derived from the microscopic constants in table 2 is given in fig. 3 in the form of a microdistribution diagram showing how the relative abundance of each protonated species depends on p[H$^+$]. It is of interest that at pH 7.4, 92.8% of spermidine is triprotonated, 4.2% protonated at both N-a and N-c, 2.4% protonated at both N-b and N-c and only 0.6% protonated at N-a and N-b. In the interactions of spermidine with the ionized phosphate groups of nucleic acids, spermidine species which are less than fully protonated may not be significant, but in its interaction with weaker bases they may well be important.

6.3. *Interactions among base sites*

Because fig. 3 describes the protonation sequence in terms of individual protonated spermi-

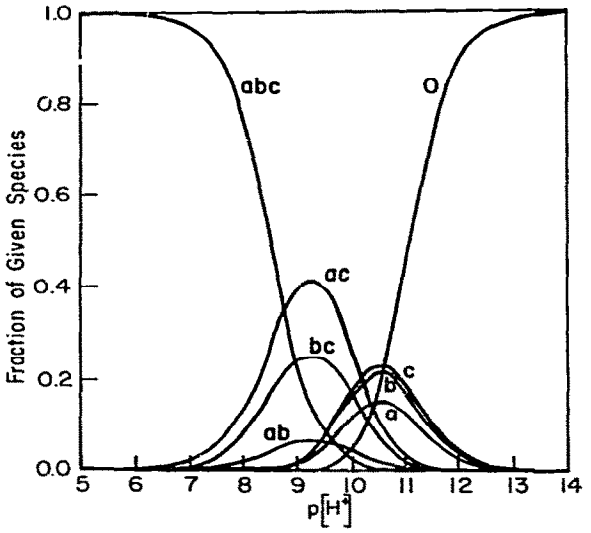

Fig. 3. Microscopic distribution diagram for spermidine calculated from the protonation constants in table 2. The labels next to each curve denote the sites that are protonated.

dine species, it does not indicate directly how the extent of protonation at each base site varies throughout the protonation sequence. This information, which reflects the base-weakening interactions among base sites, is given in fig. 4, which reports how $\bar{n}_a$, $\bar{n}_b$ and $\bar{n}_c$ vary with $\bar{n}$. For comparison, the dashed line is the average of $\bar{n}_a$, $\bar{n}_b$ and $\bar{n}_c$, i.e., the behavior that would be observed if at each stage in the protonation sequence all three

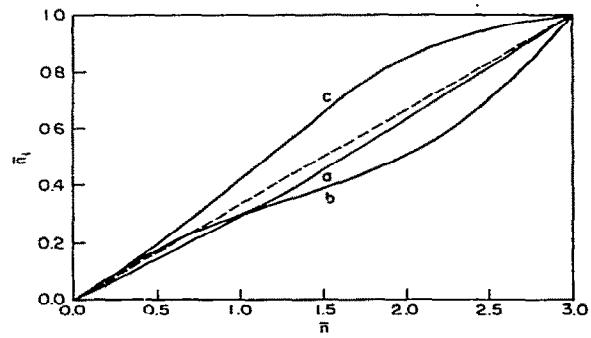

Fig. 4. The cumulative or integral basicities of N-a, N-b and N-c of sperrmidine as influenced by $\bar{n}$, the overall extent of protonation. The letter next to each curve denotes the base site.

base sites were equal in proton affinity.

Deviations of the individual $\bar{n}_i$ vs. $\bar{n}$ plots from this hypothetical average behavior reflect the relative magnitudes of the base-weakening effects of neighboring base sites. These in turn are governed primarily by the number, distance, and protonation states of the nearest neighboring nitrogens [27]. Consistent with N-c having only a single nearest neighbor four carbons distanct, $\bar{n}_c$ is substantially greater than $\bar{n}_a$ or $\bar{n}_b$ throughout the protonation sequence. Nitrogen N-a, with a single neighbor three carbons distance, is considerbly less basic than N-b. The value of $\bar{n}_a$, which increases in a nearly linear manner throughout the protonation sequence, falls just below the value for the hypothetical average base site.

Nitrogen N-b, being subject to the base-weakening effects of both N-a and N-c, exhibits a more complex protonation behavior. In the early stages of the protonation sequence, when $\bar{n}_a$ and $\bar{n}_c$ are both relatively small, $\bar{n}_b$ is slightly larger than $\bar{n}_a$. As long as $\bar{n}_c$ is small, the greater intrinsic basicity of the secondary amine outweighs the slight base-weakening effect of N-c and the protonation of N-b closely approximates that of the hypothetical average base site. As the extent of protonation at N-a and N-c increases, however, the enhanced base-weakening effects of these sites progressively suppress the basicity of N-b. As a result, the rate of increase of $\bar{n}_b$ drops and when $\bar{n}$ reaches approx. 1.2, $\bar{n}_b$ falls below $\bar{n}_a$ and remains below it for the remainder of the protonation sequence.

Because $\bar{n}_i$ at each point in the protonation sequence is based on the cumulative extent of protonation from the beginning of the protonation sequence to the point of interest, it defines the integral (or average) basicity of site i, i.e., its average basicity over the interval from $\bar{n}_i$ equal to zero to n_i equal to the value of interest. Therefore, as the value of $\bar{n}_i$ increases, it becomes progressively less sensitive to the differential (or instantaneous) basicity of the site. A direct measure of the instantaneous) basicity of the site. A direct measure of the instantaneous basicity of site i relative to that of the other base sites is $d\bar{n}_i/d\bar{n}$, the slope of the $\bar{n}_i$ vs. $\bar{n}$ plot, which for convenience we denote b_i. At each point in the protonation se-

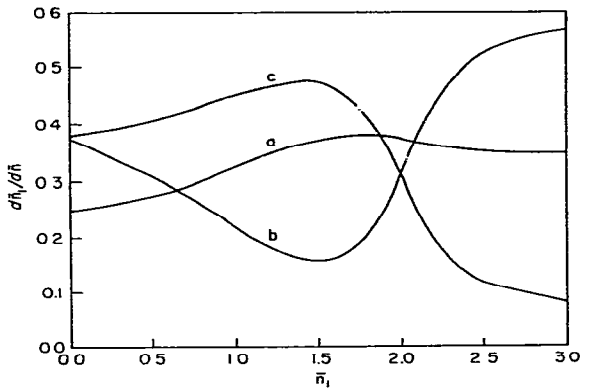

Fig. 5. The differential or instantenous basicities of N-a, N-b and N-c of spermidine as influenced by $\bar{n}$, the overall extent of protonation. The letter next to each curve indicates the base site.

quence, b_i is simply the rate of protonation of site i relative to the rate of protonation of all three base sites. That is, for an infinitessimal increase in $\bar{n}$, b_i is the fraction of that increase in bound protons which is bound at site i.

Fig. 5, which complements fig. 4, reports the dependence of b_a, b_b and b_c on $\bar{n}$. It is clear that the b_i plots of fig. 5 are indeed much more sensitive than the $\bar{n}_i$ plots of fig. 4 to the increased base-weakening effects resulting from protonation of neighboring base sites. For example, the well defined minimum at $\bar{n}$ 1.5 in the b_b curve of fig. 5 corresponds to the rather poorly defined inflection point in the n_b curve of fig. 4, and the clear maximum at $\bar{n}$ 1.5 in the b_c curve of fig. 5 has no obvious corresponding feature in the $\bar{n}_c$ curve of fig. 4.

When $\bar{n}$ is small, the values of b_i fall in the same order as do the values of $\bar{n}_i$, but as $\bar{n}$ increases, the b_i and $\bar{n}_i$ plots diverge progressively. While b_a and b_c both increase, b_c falls because of the composite base-weakening effect which progressive protonation of N-a and N-c exerts on N-b. Above $\bar{n}$ 1.5, there is a marked change in the instantaneous basicities of the sites, which is especially pronounced for N-b and N-c. The value of b_c now decreases with increasing $\bar{n}$, while that of b_b now increases, and beyond $\bar{n}$ 2.1, b_b is larger than both b_a and b_c. This increase in the instantaneous basicity of N-b beyond $\bar{n}$ 1.5 occurs because $\bar{n}_a$ and $\bar{n}_c$ are much higher than $\bar{n}_b$. For example, at $\bar{n}$ 2.1, $\bar{n}_a$, $\bar{n}_b$ and $\bar{n}_c$ are 0.68, 0.53 and 0.88, respectively, and at $\bar{n}$ 2.5, the corresponding values are 0.83, 0.72 and 0.95. Because N-a and N-c are so much more nearly fully protonated than N-b, N-b is now more able to compete for protons. By the same token, the rapid growth of $\bar{n}_b$ resulting from the increase in b_b also helps to reduce the values of b_a and b_c. The sharp drop in b_c reflects both the effect of nearly complete protonation of N-c and the increased base-weakening effect of N-b. The decrease in b_a is delayed until $\bar{n}$ exceeds 1.8 and is much smaller, because the fraction of N-a still unprotonated is significantly larger.

These indications of the relative basicities of the three base sites of spermidine and the manner in which they depend on the protonation states of neighboring nitrogens may have implications with respect to the ability of spermidine to form hydrogen bonds. As a hydrogen bond donor, nitrogen is more effective when protonated, and the weaker the basicity of the nitrogen, the stronger the hydrogen bond. Conversely, as a hydrogen bond acceptor, the most basic unprotonated nitrogen forms the strongest hydrogen bond. Thus, both the donor and the acceptor properties of the base sites of spermidine depend upon their instantaneous basicities.

Acknowledgement

The authors acknowledge with thanks the use of the nonlinear regression analysis program of H.K.J. Powell.

References

1 M. Delfini, A.L. Segre, F. Conti, R. Barbucci, V. Barone and P. Ferruti, J. Chem. Soc. Perkin Trans. 2 (1980) 900.
2 M.M. Kimberley and J.H. Goldstein, Anal. Chem. 53 (1981) 789.
3 Y. Takeda, K. Samejima, K. Nagano, M. Watanabe, H. Sugeta and Y. Kyogoku, Eur. J. Biochem. 130 (1983) 383.
4 A. Anichini, L. Fabbrizzi, R. Barbucci and A. Mastroianni, J. Chem. Soc. Dalton Trans. (1977) 2224.
5 G. Anderegg and R. Bläuenstein, Helv. Chim. Acta 65 (1982) 162.

6 J.T. Edsall, R.B. Martin and B.R. Hollingworth, Proc. Natl. Acad. Sci. U.S.A. 44 (1958) 505.
7 D.L. Rabenstein and T.L. Sayer, J. Magn. Resonance 24 (1976) 27.
8 G.C. Levy and R.L. Lichtin, Nitrogen-15 nuclear magnetic resonance spectroscopy (John Wiley and Sons, New York, 1979).
9 R.J. Kula and D.T. Sawyer, Inorg. Chem. 3 (1964) 458.
10 J.L. Sudmeier and C.N. Reilley, Anal. Chem. 36 (1964) 1707.
11 N.E. Rigler, S.P. Bag, D.E. Leyden, J.J. Sudmeier and C.N. Reilley, Anal. Chem. 37 (1965) 872.
12 D.L. Rabenstein and T.L. Sayer, Anal. Chem. 48 (1976) 1141.
13 J.L. Sudmeier and C.N. Reilley, Anal. Chem. 36 (1964) 1698.
14 J.E. Sarneski and C.N. Reilley, in: Essays on analytical chemistry, ed. E. Wanninen (Pergamon Press, Oxford, 1977) p. 35.
15 D.A. Aikens, S.C. Bunce, O.F. Onasch, H.M. Schwartz and C. Hurwitz, J. Chem. Soc. Chem. Commun. (1983) 43.
16 E.J. Herbst, D.L. Keister and R.H. Weaver, Arch. Biochem. Biophys. 75 (1958) 178.
17 G.R. Hedwig and H.K.J. Powell, Anal. Chem. 43 (1971) 1206.
18 G.R. Hedwig and H.K.J. Powell, J. Chem. Soc. Dalton Trans. (1973) 793.
19 L. Meites, Handbook of analytical chemistry (McGraw-Hill, New York, 1963) p. 1.
20 A. Bax, Two-dimensional nuclear magnetic resonance in liquids (Delft University Press, Delft, The Netherlands, 1982).
21 A. Bax and G.A. Morris, J. Magn. Resonance (1981) 42, 501.
22 N.Z. Shor, Kibernetika 13 (1977) 87 (in Russian: Translated in Cybernetics, 13 (1977) 881.
23 P. Wolfe, A bibliography for the ellipsoid algorithm (IBM, Yorktown Heights Research Center, 1980).
24 J.G. Ecker and M. Kupferschmid, Committee on Algorithms Newsletter 6 (1981).
25 J.G. Ecker and M. Kupferschmid, An ellipsoid algorithm for nonlinear programming (Rensselaer Polytechnic Institute, Troy, New York) 1981.
26 H. Kaufman, X. Xu, M. Kupferschmidt and J. Ecker, Parameter identification with the ellipsoid algorithm, Proceedings of the 1982 Conference on Information Sciences and Systems (Princeton University, Princeton, NJ, 1982).
27 D.A. Aikens, S.C. Bunce, F. Onasch, R. Parker, III, C. Hurwitz, and S. Clemans, Biophys. Chem. 17 (1983) 67.